

# Efficient antiguiding of TE and TM polarizations in low-index core waveguides without the need for an omnidirectional reflector

M. Skorobogatiy

*École Polytechnique de Montréal, Génie Physique, C.P. 6079, Centre-Ville Montreal, Québec H3C3A7, Canada*

Received June 15, 2005; revised manuscript received August 4, 2005; accepted August 5, 2005

While an omnidirectional bandgap is necessary to reflect arbitrary polarized light with a planar periodic reflector at any angle of radiation incidence, we demonstrate that omnidirectionality is not at all necessary for efficient antiguiding of modes of any polarization in low-index core photonic bandgap (PBG) fibers and waveguides. For a given radiation decay rate into the reflector and multilayer bandgap size we characterize the phase space of fiber materials leading to the same effective guiding conditions. We demonstrate that low- and high-index-contrast PBG waveguides can antiguide problematic TM-like modes equally effectively. Finally, the possibility of TE-like guidance of a TM-polarized mode is described. © 2005 Optical Society of America

OCIS codes: 060.2400, 130.2790.

Antiguiding fibers and waveguides promise important advantages over standard total-internal-reflection fibers in various applications. Particularly, hollow photonic bandgap (PBG) fibers such as Bragg fibers,<sup>1,2</sup> microstructured fibers,<sup>3,4</sup> and multilayer planar waveguides,<sup>5-7</sup> are able to guide light through hollow (gaseous) cores, promising low material loss and nonlinearity and achieving radiation confinement via reflection from a surrounding dielectric multilayer mirror. Examples of potential applications of hollow PBG fibers are high-power guiding at a designable wavelength, ultralow nonlinearity fibers for telecommunications, and compact sensors for which functional materials could be integrated directly into the hollow fiber core. Antiguiding waveguides can also prove to be important in guiding through low-refractive-index liquids such as water, which is important in biological sensing and chemical characterization applications,<sup>8</sup> opening the prospect of building liquid-core waveguides on a chip. Until recently Teflon AF was the only solid material available as a lower-index cladding for a water core, thus making a total-internal-reflection, liquid-core waveguide possible.

In Ref. 9 the principle of omnidirectional (OD) reflectivity was described, stating that a planar multilayer made of a periodic sequence of bilayers of two different dielectrics can be designed to completely reflect incoming light in a certain frequency range for any angle of incidence and any state of polarization. The recipe was a choice of high enough index contrast between bilayer dielectrics, as well as high enough difference between reflector refractive indices and a core index. It is frequently suggested that to build an efficient antiresonant waveguide effective for both TE- and TM-polarized modes (TM being most problematic) one needs an OD reflector as a part of the design. Although this statement is easy to rebuff with the counterexample of hollow silica-based microstructured fibers<sup>4</sup> that guide with non-OD reflectors, the question of antiresonant waveguide guiding efficiency as a function of core and reflector indices is an interesting one. Particularly, in large-

core two-dimensional waveguides and Bragg fibers the ray picture of guiding is applicable when a well-defined angle of incidence onto a reflector can be assigned to a core mode, thus envisioning its propagation by consecutive reflections from a PBG mirror. In this regime, to guarantee low-loss guiding it is necessary to design an efficient reflector for all polarizations but only a narrow range of incidence angles around an effective incidence angle of a core mode. This design condition is considerably less restrictive than that of OD reflection. The efficiency of a reflector operating inside a bandgap can be characterized by the radiation decay rate per bilayer, which also defines waveguide absorption and radiation losses as well as the size of the reflector bandgap. The reflector bandgap defines waveguide spectral properties as well as resistance to perturbations.

In this Letter we consider the performance of reflectors made of a periodic sequence of dielectric layers, as encountered in Bragg fibers and planar waveguides. We first present design considerations for an optimal two-material periodic reflector operating at a fixed angle of incidence. Then we characterize reflector performance in terms of a field decay rate and a bandgap size for both TE and TM polarizations. We then consider low-refractive-index core planar waveguides and Bragg fibers and demonstrate that two distinct guiding regimes exist for a problematic TM polarization, one of them being TE like. In Fig. 1(a) a schematic is presented of a semi-infinite reflector made of a periodic sequence of high- ( $n_h$ ) and low- ( $n_l$ ) refractive-index bilayers with corresponding layer thicknesses  $d_h$  and  $d_l$ . The angle of radiation incidence is fixed and equal to  $\theta$ . The refractive index of the material above the reflector (the core material) is  $n_c$ . The wave-vector component along the  $z$  direction  $k_z = \omega n_c \sin(\theta)$  is conserved throughout the reflector, while its  $x$  component in a layer of refractive index  $n$  is  $k_x^n = \omega \sqrt{n^2 - n_c^2 \sin^2(\theta)}$ . In each layer,  $y$  field components can be represented in the form of two counter-propagating waves  $[A_j^1 \exp(-ik_x^n x) + A_j^2 \exp(ik_x^n x)] \times \exp(ik_z z - i\omega t)$ , where  $j$  is a layer index, with  $j=0$

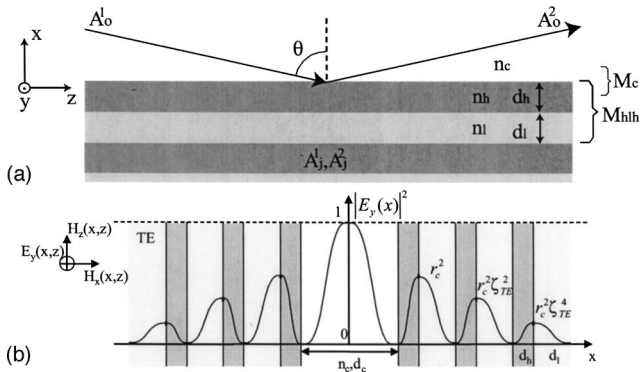


Fig. 1. Schematics of (a) a planar PBG reflector, (b) a planar hollow PBG waveguide and a fundamental TE mode.

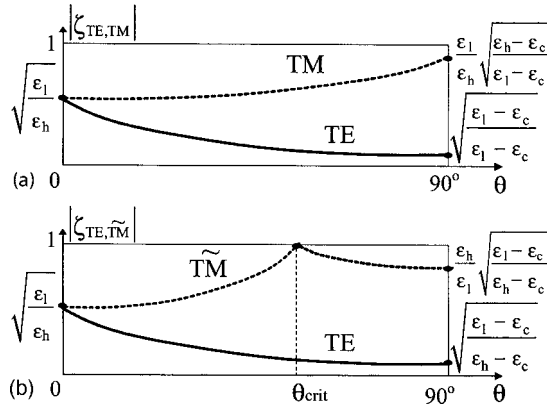


Fig. 2. Schematics of TE and TM radiation decay rates into the quarter-wave stack reflector optimized for an incidence angle  $\theta$  when (a)  $\epsilon_c < \epsilon_{\text{crit}}$ , (b)  $\epsilon_c > \epsilon_{\text{crit}}$ .

corresponding to the core material. Standard transfer matrix theory<sup>10</sup> can be used to relate expansion coefficients in layers  $j$  and 0. Thus, defining the core high-index layer transfer matrix as  $M_{\text{ch}}$  and the bi-layer transfer matrix as  $M_{\text{hlh}}$ , we can, for example, write the field coefficients in the high-index layer  $j+1$  as  $\bar{A}_j = (M_{\text{hlh}})^{j/2} M_{\text{ch}} \bar{A}_0$ . Assuming an infinite number of layers in the reflector and requiring expansion coefficients  $\bar{A}_j$  to tend to zero as  $j \rightarrow \infty$ , we arrive at the conclusion that  $M_{\text{ch}} \bar{A}_0$  has to be proportional to an eigenvector of matrix  $M_{\text{hlh}}$  with a corresponding eigenvalue  $\zeta_{<1}$  of a magnitude smaller than 1. The eigenvalue itself will determine the field decay rate into the reflector per bilayer as  $\bar{A}_j \sim \zeta_{<1}^{j/2} \bar{A}_0$ ; thus, the smaller the eigenvalue, the smaller will be the field penetration into the multilayer. From an analytical expression for  $\zeta_{<1}$ , it follows that, for a fixed angle, to minimize the value of  $\zeta_{<1}$  at a center wavelength  $\lambda_c$ , the optical thicknesses of individual layers at such a wavelength will have to satisfy the quarter-wave condition  $d_h k_x^{n_h} = d_l k_x^{n_l} = \pi/2 \times (2n+1)$ , where  $n$  is an integer.

For such an optimal reflector the field decay rate can be found analytically, and for TE polarization (where the electric field is parallel to the reflector plane) it is  $|\zeta_{\text{TE}}| = k_x^{n_l} / k_x^{n_h}$ . In Fig. 2(a) a schematic of a TE field decay rate is presented, featuring monotoni-

cally increasing reflector efficiency for oblique angles of incidence. Reflection of TM polarization (where the magnetic field is parallel to the reflector plane) is more challenging, and, depending upon the value of the core index, two cases are possible. If  $\epsilon_c < \epsilon_{\text{crit}}$  (TM regime), where  $\epsilon_{\text{crit}} = \epsilon_h \epsilon_l / (\epsilon_h + \epsilon_l)$ , one finds that  $|\zeta_{\text{TM}}| = (\epsilon_l k_x^{n_h}) / (\epsilon_h k_x^{n_l})$ , which is presented in Fig. 2(a). While reflection of TM polarization is worse than reflection of TE polarization for any angle of incidence, one can still design a reflector that reflects both polarizations as  $|\zeta_{\text{TM, TE}}| < 1$  for any design angle  $\theta$ . If  $\epsilon_{\text{crit}} < \epsilon_c < \epsilon_l$  ( $\tilde{\text{TM}}$  regime), then  $|\zeta_{\text{TM}}| = (\epsilon_h k_x^{n_l}) / (\epsilon_l k_x^{n_h})$ , which is plotted in Fig. 2(b). As before, reflection of TM polarization is worse than reflection of TE polarization; moreover, there exists an incidence angle  $\theta_{\text{crit}} = \sin^{-1}(\epsilon_{\text{crit}} / \epsilon_c)$  for which it is impossible to design an efficient reflector, as  $|\zeta_{\text{TM}}(\theta_{\text{crit}})| = 1$ .

We now consider the performance of reflectors for oblique incidence angles  $\theta \sim 90^\circ$ ,  $k_z \sim \omega n_c$ , which is relevant for modal propagation in planar waveguides with large enough cores [Fig. 1(b)] and for Bragg fibers.<sup>11</sup> We find that for a wavelength  $\lambda$  this condition is typically satisfied when  $d_c \geq 10\lambda$ . To characterize the antiguiding efficiency of a large-core waveguide, in Fig. 3(a) we present universal contour plots of the radiation decay rates into the reflector for TE and TM polarizations as functions of the relative multilayer indices (with respect to  $n_c$ ) at  $\theta \sim 90^\circ$ . Note that for TM polarization there are two distinct regions of phase space, in Fig. 3(a) denoted as TM when  $\epsilon_c < \epsilon_{\text{crit}}$  and  $\tilde{\text{TM}}$  when  $\epsilon_{\text{crit}} < \epsilon_c < \epsilon_l$ . In each of the regions we present contour lines of material parameters corresponding to the same field decay rate. For example, a polymer-based low-index-contrast reflector with  $n_l = 1.414$  and  $n_h = 1.6$ , antiguiding (in the  $\tilde{\text{TM}}$  regime), in a liquid-core ( $n_c = 1.32$ ) will have the same TM field decay rate of  $\sim 0.72$  per bilayer as a

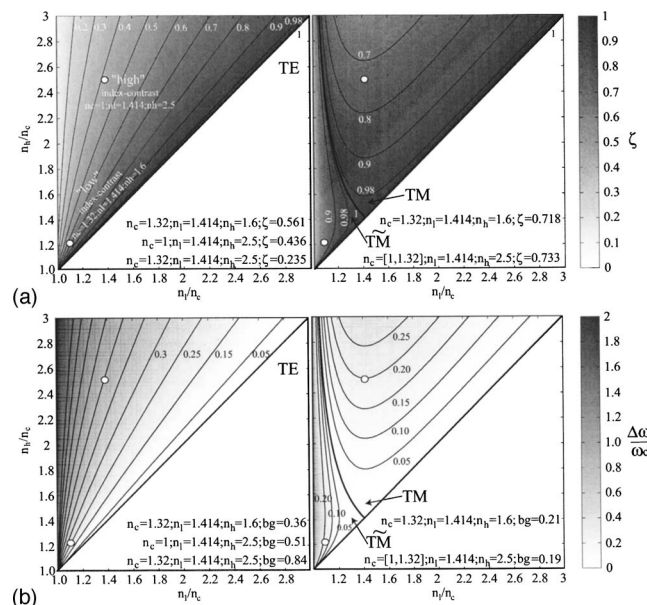


Fig. 3. TE, TM polarizations,  $\theta \sim 90^\circ$ . Circles, examples of high and low index contrast. (a) Field decay rates into the reflector. (b) Relative bandgap sizes.

high-index-contrast OD reflector with indexes  $n_l = 1.414$  and  $n_h = 2.5$ , guiding (in the TM regime) in air ( $n_c = 1$ ) or in liquid ( $n_c = 1.32$ ).

Another important reflector characteristic is a bandgap size. We consider  $(k_z, \omega)$  to be on the edge of a bandgap if the corresponding eigenvalue of a bilayer transfer matrix  $\zeta_{<1} = 1$ , thus rendering the reflector ineffective. For an optimal quarter-wave stack designed for a particular angle of radiation incidence  $\theta$  and a center wavelength  $\lambda_c$ , the size of the fundamental bandgap along the line  $k_z = \omega n_c \sin(\theta)$  (the distance along this line between the two bandgap edges) can be found analytically and is given by  $\Delta\omega/\omega_c = 4/\pi \sin^{-1}[\sqrt{(\eta-1)/(\eta+1)}]$ , where  $\eta = (\zeta_{<1} + \zeta_{<1}^{-1})/2$ .  $\zeta_{<1}$  is evaluated at  $\lambda_c$  and  $\theta$  and is given by the expressions in the previous paragraphs. In large-core waveguides  $\theta \sim 90^\circ$ , and  $k_z = \omega n_c$  defines an approximate dispersion relation of the low-loss core modes. Thus, the bandgap size given by the above expression at  $\theta \sim 90^\circ$  will be the one along the dispersion curve of a mode. In Fig. 3(b) we present universal contour plots of the reflector bandgaps for TE and TM polarizations at  $\theta = 90^\circ$  as functions of the relative multilayer indices. From the figure one can see that low-index-contrast non-OD and high-index-contrast OD reflectors discussed above exhibit similar TM bandgaps of  $\sim 20\%$ .

Finally, we investigate the field distribution of TE- and TM-polarized fundamental modes in a low-index-core planar waveguide for which  $d_c k_x^{n_c} = \pi$ . In Fig. 1(b) the field distribution of a TE-polarized mode is shown, where  $r_c \approx \lambda / (2d_c \sqrt{\epsilon_h - \epsilon_l})$ , when  $d_c \gg \lambda$ . Because of the  $r_c^2$  prefactor, the outgoing flux in the reflector (which defines the radiation leakage through a finite size reflector), as well as the amount of field energy in the reflectors (which defines waveguide loss due to the material absorption) decreases with core size as  $d_c^{-3}$  when normalized by the total energy in the mode. Such scaling of material absorption and radiation losses is also observed in TE<sub>0n</sub> modes of hollow Bragg fibers.<sup>11</sup> On the other hand, for TM-polarized modes two field distributions are possible, depending on whether operation is in the TM or  $\tilde{\text{TM}}$  regimes. In Fig. 4(c) distributions of magnetic (solid curves) and electric (dotted curves) fields are presented, where  $|E_z^{\text{core}}(x)| \ll |E_x^{\text{core}}(x)| \approx |H_y^{\text{core}}(x)|/n_c$ . In the TM regime, field content in the core is considerably different from that in the TE case, leading to  $d_c^{-1}$  scaling of radiation and absorption losses with the core size, which is similar to the scaling of HE, EH modal losses in hollow Bragg fibers.<sup>11</sup> On the other hand, in the  $\tilde{\text{TM}}$  regime field distribution in the core becomes similar to that of a TE case, thus leading again to a  $d_c^{-3}$  dependence of radiation and absorption losses even for a TM polarized mode! This analytical result for planar reflectors also holds for antiguiding Bragg fibers. In Fig. 4(a) we present TM radiation loss of a 31-layer Bragg fiber designed for  $\lambda_c = 1 \mu\text{m}$  with  $n_h = 2.5$ ,  $n_l = n_{\text{clad}} = 1.414$  as a function of a core radius. This high-

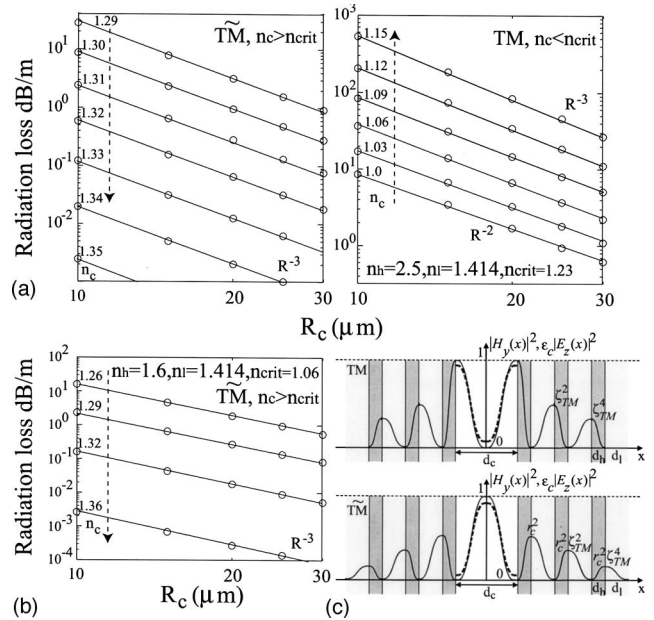


Fig. 4. TM and  $\tilde{\text{TM}}$  regimes. (a) High index contrast. (b) Low index contrast, Bragg fibers. (c) Field distributions in antiguiding planar waveguides.

index-contrast fiber exhibits OD reflectivity when  $n_c = 1$ . In the TM regime with  $n_c < 1.23$  one can observe variable radiation loss scaling with core size  $\sim R^{-2} - R^{-3}$ , while in the  $\tilde{\text{TM}}$  regime with  $n_c > 1.23$  this scaling becomes  $R^{-3}$ . In Fig. 4(b) TM radiation loss in low-index-contrast fiber operated in the  $\tilde{\text{TM}}$  regime is presented. The same number of layers is assumed, with  $n_h = 1.6$ ,  $n_l = n_{\text{clad}} = 1.414$ . Note the  $R^{-3}$  scaling of radiation losses. As established earlier, a high-index-contrast reflector operating with  $n_c = 1$ , 1.32 has field decay factor and bandgap size very similar to a low-index contrast reflector operating with  $n_c = 1.32$ , thus leading to the comparable TM radiation losses for both of these Bragg fiber designs.

## References

1. B. Temelkuran, S. D. Hart, G. Benoit, J. D. Joannopoulos, and Y. Fink, *Nature* **420**, 650 (2002).
2. T. Katagiri, Y. Matsuura, and M. Miyagi, *Opt. Lett.* **29**, 557 (2004).
3. C. M. Smith, N. Venkataraman, M. T. Gallagher, D. Muller, J. A. West, N. F. Borrelli, D. C. Allan, and K. W. Koch, *Nature* **424**, 657 (2003).
4. P. Russell, *Science* **299**, 358 (2003).
5. S. S. Lo, M. S. Wang, and C. C. Chen, *Opt. Express* **12**, 6589 (2004).
6. Y. Yi, S. Akiyama, P. Bermel, X. Duan, and L. C. Kimerling, *Opt. Express* **12**, 4775 (2004).
7. J. M. Fini, *Meas. Sci. Technol.* **15**, 1120 (2004).
8. T. Dallas and P. K. Dasgupta, *TrAC, Trends Anal. Chem.* **23**, 385 (2004).
9. J. N. Winn, Y. Fink, S. Fan, and J. D. Joannopoulos, *Opt. Lett.* **23**, 1573 (1998).
10. P. Yeh, *Optical Waves in Layered Media* (Wiley, 1988).
11. S. G. Johnson, M. Ibanescu, M. Skorobogatiy, O. Weisberg, T. D. Engeness, M. Soljačić, S. A. Jacobs, J. D. Joannopoulos, and Y. Fink, *Opt. Express* **9**, 748 (2001).